

Blueshift Plasmonic effect in photonic crystal cavity with gold nano-structure

Ashish Yadav (✉ ashish84yadav@gmail.com)

Shandong University of Technology

Yongling Wu

Shandong University of Technology

Zheng Hongyu

Shandong University of Technology

Neha Yadav

Shandong University of Technology

Research Article

Keywords: Colloidal spheres, self-assembly, plasmonic, nano-cavity, laserspectroscopy, spontaneous emission

Posted Date: February 26th, 2021

DOI: <https://doi.org/10.21203/rs.3.rs-243917/v1>

License:   This work is licensed under a Creative Commons Attribution 4.0 International License.

[Read Full License](#)

Abstract

In this research article, we report the plasmonic effect exhibited by a self-assembled photonic crystal cavity in nanostructures using a second harmonic laser exposure. The photonic nanostructures composed of gold nanoparticles (AuNPs), enhanced the fluorescence properties which undergo into lattice planes and thereby affect the nonlinear properties. The newly fabricated colloidal structures exhibited a strong plasmonic interaction with different laser power density. The outcome of this research presents the self-assembled nano-photonic cavity as a suitable plasmonic nanostructure for optoelectronic applications. These nanostructures can be fabricated using high power laser source, e.g. dye laser and solid-state laser.

Introduction

Much interest has been shown in the field of colloidal spheres (CS) during the past few years, by the scientific community, because of their unique, challenging and potential applications in optoelectronics [1]. The dependence of optical, magnetic, physical and chemical properties on the size and shape of optical nano-materials have drawn significant attention for new applications of photonic crystals and colloidal spheres for several different technological areas [2]. Laser light interaction with the colloidal sphere (CS) increases the high-quality factors for optical devices and the efficiency of lasers [3, 4]. CS has proved their wide applications in several optoelectronic fields [5-7]. The resultant or the collective oscillations of available free electrons within nanoparticles, along with localized surface plasmon resonance (LSPR) band, may tune the optical characteristics of metal nanoparticles. According to previous findings, the skillful variation of the size and shape of the nanoparticles may tune the LSPR band in visible and near-infrared [8]. Attachment of colloidal spheres with gold nanoparticles (AuNPs) may also highly manipulate the fluorescence intensity of dye [9]. Some exceptional properties originating from surface modification and quantum confinement prove CS a useful candidate in nanotechnology [10, 11]. The AuNPs can induce self-organization into lattice planes [12-14]. This system is required to control the positioning of the metal nanoparticles in the crystal plane [7, 15]. According to literature, nonlinear responses are reported to be enhanced because of the strong interaction of plasmonic AuNP [16, 17]. This variety of nanoparticle assemblies is wholly different and paves a new way for new possible meta-materials having the desired optical and electronic properties, which can be tuned by the size of colloidal particles and LSPR [18]. Within these LSPRs, the oscillations of collective electrons fall in the metal conduction band and can be modified by an external field by employing closely spaced metallic nanoparticles (MNPs).

LSPR is the exceptional optical properties of MNPs. As compared to the identical dimensions of dielectric NPs, MNPs possess a larger cross-section of scattering than that of the NPs. The surface plasmon resonance (SPR) is a unique characteristic property of MNPs, by which the light waves can be confined close to the surface of nanoparticles and a high gain can be achieved. [19]. The nature of the material, its shape and size along with the nearby environment of NPs, can decide the position of SPR. The NPs can modify the transition rates (non-radiative and radiative) of the dye molecules in the vicinity [20-23].

Within the present work, we have examined the laser interaction performance with polymer-based colloidal spheres (CS), attached with AuNPs, doped with dye pigment Rhodamine 6G (Rh6G). A blue plasmonic shift at high tuning laser power density was obtained. The Colloidal spheres CS-Rh6G attached with AuNPs exhibited strong interaction with fluorescence and peak broadening, which in turn, clearly indicates blue plasmonic behavior. This behavior depends on laser power density instead of CS-Rh 6G. The CS-Rh 6G-AuNPs also demonstrated peak broadening and improved spontaneous emission properties. These results suggested that the self-assembled CS-Rh6G-AuNPs nano-photonics systems can be used for the future application of several optoelectronic areas.

Materials And Methods

Synthesis & attachment of colloidal spheres with gold nanoparticles:

Monodisperse polymer-based colloidal spheres were synthesized by emulsion polymerization method. Polymethyl methacrylate (PMMA) spheres were chemically synthesized by adding 25 mL monomer and 200 mL water in a three-necked flask containing dye solution (10×10^{-4} M) at 900 rpm stirring speed. The mixture was rinsed to reflux, and after reaching to 90°C of the mixture, potassium persulfate powder (0.02 gm to 0.2 gm) was dissolved in the solution. After 120 minutes, the reaction was paused. The solution was cooled down until room temperature then silica wool was used to filter the colloidal solution. Chemical reduction method was used to synthesize AuNPs, in which, 5 mL solution of chloroauric acid ($\text{HAuCl}_4 \cdot 3\text{H}_2\text{O}$) having a concentration of 10 mM was heated until boiling in 100 mL beaker with 90 mL deionized water and stirring at 400 rpm. 5 mL of 3.8×10^{-2} M trisodium citrate dihydrate ($\text{Na}_3\text{C}_6\text{H}_5\text{O}_7 \cdot 2\text{H}_2\text{O}$) was further added into the solution. The solution changed color within 15 minutes similar to red wine, while at continuous stirring. 10 mL of colloidal spheres and some amount of PVP was added into the solution, it was continuously stirred overnight and then was washed with water 3 times. AuNPs were attached to photonic crystals by adding some amount of the AuNPs after centrifugation. Finally, the mixture was aged for 24 hrs.

Results

For characterization, we synthesized CS with dye molecules, some amount of AuNPs was added and after that, a continuous stirring for 10 hours was done. Finally, the solution of CS and Au NPs was spread over the silicon substrate and left for getting a dry surface in figure 1.

Figure 2, showing scanning electron microscope images, which are typical close packing arrangements. The self-assembly of CS well ordered. In addition, their diameters as 300 nm for CS-Rh6G and 20 nm AuNPs. AuNPs distributed in superlattice plane on CS. **Fig.2a** shows well-ordered PMMA CS with few defects and **fig.2b** shows well organized AuNPs on PCs. Bright tiny particles are AuNPs.

Experiment set-up for laser characteristic

Optical effect was observed by the second harmonic generation laser such as Nd:YAG at a repetition rate of 20 kHz and pulse duration of 1 ns. The sample was fixed at a circular platform to allow the detection of the luminescence around the particles. A notch filter filtered the collected emission.

The measurements were performed by changing the excitation power from small to large values. The energy transfer between the dye molecule and metal nanoparticles (Förster resonance energy transfer, FRET) [24, 25] and surface energy transfer (SET) [26-28] was explained using Förster's elegant theory.

$$E = \frac{1}{1 + (r/R_0)^6} \quad (1)$$

The value of E depends on the separation distance r between donor-to-acceptor and varies with an inverse 6th-power law because of the dipole-dipole coupling mechanism. R_0 denotes the Förster distance of this donor-acceptor pair [29, 30]. However, the conventional FRET technique suffers from many limitations and can be employed only on dye molecules as donor and acceptor. The energy transfer beyond this distance becomes too weak to measure [31, 32]. In this process, dye molecules take part in the resonance energy transfer and affect the optical traits of donor and acceptor molecules.

MNPs are reported to influence the radiative rate of a chromophore [33, 34]. Fluorescence intensity can be enhanced by a modification of the chromophore radiation rate by the AuNPs. The variation of the radiative rate of chromophore has already been explained in the context of the coupling of the molecular and nanoparticle dipoles. The rates of decay for radiative and non-radiative decay depend on the chromophore dipole related to the surface of the particle [35]. During the enhancement of laser power, the radiative transition enhanced and a little shift towards the lower side [36] was observed. Timmerman et al. reported the power dependence shift of spectral peaks with different sizes of particles [37]. In this paper, laser light interaction with CS attached with dye molecules, attached with Au-NPs at different powers is studied. The more is the power of laser, the more energy is absorbed by CS and hence the more is the emission by the composite. The blue shift in the spectrum is attributed to the absorption at higher energy radiation and emission from the adjacent attached CS and AuNPs. However, for increased power (50 to 275 mW) of laser, with Rh 6G dye-doped CS, neither blue shift at high power nor peak broadening was observed (Fig. 4). This effect clearly shows the plasmonic optical effects on CS-Rh6G+AuNPs, peak shift and peak broadening associated with the attachment of the AuNPs with CS. The peak broadening is recorded to augment first, a reduction after a specific power of the laser, followed by a saturation [38, 39].

Table 1. Comparative study of spontaneous Emission spectrum in colloidal spheres with dye molecules and without the attachment of metal nanoparticles.

Power (X-Axis)	FWHM (Y-Axis) With dye	FWHM (Y-Axis) With Au-NPs
50 mW	53 nm	90 nm
75 mW	53 nm	90 nm
100 mW	53 nm	90 nm
125 mW	53 nm	94 nm
150 mW	53 nm	97 nm
175 mW	53 nm	99 nm
200 mW	53 nm	102 nm
225 mW	53 nm	102 nm
250 mW	53 nm	102 nm
275 mW	53 nm	98 nm

In table 1, the variation in FWHM (Y-Axis) with laser power (X-Axis) has been shown. The emission spectrum at different pump powers was recorded, and changes in FWHM of the spectrum was observed.

Colloidal based self-assembly film was excited by laser radiation, the probability of radiative transition increases at higher energy edge of the spectrum, creating a blue shift in the recorded spectrum [40], while enhancing the pump power from 50 to 275 mW. It indicates that the laser powers affect the peak broadening and peak shift [41], as has been shown in **fig. 3**. With the increased pump power, the gain in the proximity of peak emission wavelength increases, attributing to a blue shift towards the maximum of the emission spectrum. This gain, for an inhomogeneous medium, at any wavelength equals to the product of cross-section of stimulated emission and difference of population density, as follows:

$$g_{\lambda}^D = \Delta N_{ul} \sigma_{ul}^D(\lambda) \quad (2)$$

Where g_{λ}^D is the gain at any wavelength, ΔN_{ul} is the difference in population density, and $\sigma_{ul}^D(\lambda)$ is the cross-section of stimulated emission.

CS-RhB+AuNPs are involved in the emission process; hence, the difference in population density is higher for higher pump powers. This will enhance the gain in the proximity of the peak wavelength of the emission, which in turn leads to a relative blue shift in the emission spectrum towards the maximum of emission. The increment in pump power beyond does not produce any further blue shift in the emission spectrum, probably because of gain saturation. In various studies, almost identical relative blueshifts have been observed towards the peak of emission cross-section, while increasing the pump power. Within this study, the CS surface was modified with AuNPs and photoluminescence, higher than without AuNPs was observed (**Fig. 5**). Gontijo et al. reported that the modification in the density of surface plasmon states is necessary to increase the rate of spontaneous emission and simultaneously to enhance the quantum efficiency of the semiconductor materials being used in the reaction [38]. The excitation of plasmons can be controlled by surface Plasmon density of states and this configuration is essential to increase the properties of luminescence [42].

The emission spectrum in **fig.5a** indicates a high PL intensity with and without AuNPs in the CS Rh6G surface. This PL enhancement is due to the attachment of AuNPs. Experimental and theoretical compression UV spectrum are shown in **fig.5b**. **Fig. 5d** shows, energy level diagram of CS-Rh 6G AuNPs, excited by the wavelength of 532 nm. The lower shift occurs due to the Intersystem crossing (ISC). The peak shifting and peak broadening are attributed to the plasmonic effect due to AuNPs self-assembly.

Experimental and simulation study of absorption spectrum CS-Rh6G and CS-Rh6G AuNPs (**a** and **b**). Simulation studies and experimental data are following each other and show a good fitting. The distinct gold surface plasmonic peak is observed at ~522 nm in gold attached samples (**c**). Time-resolved fluorescence spectrum of the Rh6G-CS and presence of AuNPs, and energy transfer diagram (**d**).

$$k_T(r) = \frac{1}{\tau_D} \left(\frac{R_0}{r} \right)^6 \quad (3)$$

where τ_D is the lifetime of the donor in the absence of the acceptor, r is the distance between the donor-acceptor pair, and R_0 is the Förster distance, at which the transfer rate $k_T(r)$ becomes equal to the decay rate of the donor while the donor is absent. Chance et al. [44] termed the rate of energy transfer from a dye molecule to the surface of the metal as surface energy transfer (SET).

The average size of AuNPs was calculated to be 20 nm by SEM. All of the AuNPs were spherically symmetric. Blue shift occurrence is indicative of the capping of nanoparticles with the stabilization molecule [45]. The plasmon resonance band for gold nanoparticle is not only dependent on the particle size but also the surrounding medium's dielectric constant. When we change the stabilization molecule, probably the dielectric constant also changes and therefore, it causes a shift at the band.

Conclusions

In summary, this research explained the encapsulation of dye molecules with colloidal spheres and AuNPs using a self-assembly approach. Further, the blue shift plasmonic effect exhibited by plasmonic nano-cavity fabricated was investigated to be due to the self-assembly of AuNP. It is observed that by varying the laser powers, colloidal spheres with AuNPs exhibited a shift from shorter to greater wavelengths at high power along with a peak shifting as compared to CS-Rh 6G specimen. This new 3D-CS material may be suitable for several nonlinear optical devices and other laser applications.

Abbreviations

colloidal spheres (CS), Polymethyl methacrylate (PMMA), localized surface plasmon resonance (LSPR), gold nanoparticles (AuNPs),

Declarations

Availability of data and materials:

All data generated or analyzed during this study are included in this article

Authors' contributions

AY carried out plasmonic behavior in nanostructures and drafted the manuscript. VA synthesized metal nanoparticles part of this manuscript. AK, YW, ZH and SR discussed and helped draft the manuscript. All authors read and approved the final manuscript.

Author's Details :

¹Center for advanced laser manufacturing (CALM), Shandong university of technology, Zibo, 255000, P.R. China. ²School of Physics, Southeast University, Jiangning District, Nanjing 211189, People's Republic of China. ³NanoBioTech Laboratory, Department of Natural Sciences, Division of Sciences, Art, & Mathematics, Florida Polytechnic University, Lakeland, USA. ⁴Nanoscience and Nanotechnology Initiative, National University of Singapore, 10 Kent Ridge Crescent 119260, Singapore.

Competing interests:

The authors declare that they have no competing interests.

Funding:

This study was supported by Mechanical engineering department, Shandong university of Technology, Zibo, China. The Program Taishan Scholar scheme of Shandong Province, China (ts 20190401).

Acknowledgment:

Y.W. and Z.H. acknowledge the financial support from from the Taishan Scholar scheme of Shandong Province, China (ts 20190401).

Corresponding Author: Email: - ashish84yadav@gmail.com (A.Y.)

References

1. Cersonsky, R.K., et al., *Relevance of packing to colloidal self-assembly*. Proceedings of the National Academy of Sciences, 2018. **115**(7): p. 1439-1444.
2. Promnimit, S., et al. *Growth Process of Novel Thin Films by Directed Self Organization of Nanoparticles*. in *2007 2nd IEEE International Conference on Nano/Micro Engineered and Molecular Systems*. 2007.

3. Tandaechanurat, A., et al., *Lasing oscillation in a three-dimensional photonic crystal nanocavity with a complete bandgap*. Nature Photonics, 2011. **5**(2): p. 91-94.
4. Noda, S., M. Fujita, and T. Asano, *Spontaneous-emission control by photonic crystals and nanocavities*. Nature Photonics, 2007. **1**(8): p. 449-458.
5. Tame, M.S., et al., *Quantum plasmonics*. Nature Physics, 2013. **9**(6): p. 329-340.
6. Oulton, R.F., et al., *Plasmon lasers at deep subwavelength scale*. Nature, 2009. **461**(7264): p. 629-632.
7. Huang, C.-p., et al., *Long-Wavelength Optical Properties of a Plasmonic Crystal*. Physical Review Letters, 2010. **104**(1): p. 016402.
8. Genov, D.A., et al., *Anomalous spectral scaling of light emission rates in low-dimensional metallic nanostructures*. Physical Review B, 2011. **83**(24): p. 245312.
9. Park, D.J., et al., *Plasmonic photonic crystals realized through DNA-programmable assembly*. Proceedings of the National Academy of Sciences, 2015. **112**(4): p. 977.
10. Cheng, X., et al., *Colloidal silicon quantum dots: from preparation to the modification of self-assembled monolayers (SAMs) for bio-applications*. Chem Soc Rev, 2014. **43**(8): p. 2680-700.
11. Banik, B.L., P. Fattahi, and J.L. Brown, *Polymeric nanoparticles: the future of nanomedicine*. WIREs Nanomedicine and Nanobiotechnology, 2016. **8**(2): p. 271-299.
12. Venditti, I., *Gold Nanoparticles in Photonic Crystals Applications: A Review*. Materials, 2017. **10**(2): p. 97.
13. Guzman, E., et al., *Polymer-surfactant systems in bulk and at fluid interfaces*. Adv Colloid Interface Sci, 2016. **233**: p. 38-64.
14. Chen, G., et al., *Fluorescence Enhancement on Large Area Self-Assembled Plasmonic-3D Photonic Crystals*. Small, 2017. **13**(9).
15. Liang, J., et al., *Near-infrared tunable multiple broadband perfect absorber base on VO₂ semi-shell arrays photonic microstructure and gold reflector*. Materials Research Express, 2018. **5**(1): p. 015802.
16. Ding, S.-J., et al., *Largely Enhanced Saturable Absorption of a Complex of Plasmonic and Molecular-Like Au Nanocrystals*. Scientific Reports, 2015. **5**(1): p. 9735.
17. Nan, F., et al., *Tunable Plasmon Enhancement of Gold/Semiconductor Core/Shell Hetero-Nanorods with Site-Selectively Grown Shell*. Advanced Optical Materials, 2014. **2**(7): p. 679-686.
18. Peter, J., et al., *Pumping scheme dependent multimode laser emission from free-standing cylindrical microcavity*. Optics Communications, 2014. **320**: p. 125-128.
19. Lawandy, N.M., et al., *Laser action in strongly scattering media*. Nature, 1994. **368**(6470): p. 436-438.
20. Dulkeith, E., et al., *Fluorescence Quenching of Dye Molecules near Gold Nanoparticles: Radiative and Nonradiative Effects*. Physical Review Letters, 2002. **89**(20): p. 203002.
21. Yadav, A., et al., *Tunable random lasing behavior in plasmonic nanostructures*. Nano Convergence, 2017. **4**(1): p. 1.

22. Khatua, S., et al., *Resonant Plasmonic Enhancement of Single-Molecule Fluorescence by Individual Gold Nanorods*. ACS Nano, 2014. **8**(5): p. 4440-4449.
23. Ziegler, J., et al., *Gold nanostars for random lasing enhancement*. Optics Express, 2015. **23**(12): p. 15152-15159.
24. *Front Matter*, in *FRET – Förster Resonance Energy Transfer*. p. i-xxii.
25. *Förster Theory*, in *FRET – Förster Resonance Energy Transfer*. p. 23-62.
26. *Fluorescence Anisotropy*, in *Principles of Fluorescence Spectroscopy*, J.R. Lakowicz, Editor. 2006, Springer US: Boston, MA. p. 353-382.
27. Yun, C.S., et al., *Nanometal surface energy transfer in optical rulers, breaking the FRET barrier*. J Am Chem Soc, 2005. **127**(9): p. 3115-9.
28. Jennings, T.L., M.P. Singh, and G.F. Strouse, *Fluorescent Lifetime Quenching near $d = 1.5$ nm Gold Nanoparticles: Probing NSET Validity*. Journal of the American Chemical Society, 2006. **128**(16): p. 5462-5467.
29. Corry, B., D. Jayatilaka, and P. Rigby, *A Flexible Approach to the Calculation of Resonance Energy Transfer Efficiency between Multiple Donors and Acceptors in Complex Geometries*. Biophysical Journal, 2005. **89**(6): p. 3822-3836.
30. Melle, S., et al., *Förster Resonance Energy Transfer Distance Dependence from Upconverting Nanoparticles to Quantum Dots*. The Journal of Physical Chemistry C, 2018. **122**(32): p. 18751-18758.
31. Lakowicz, J.R., *Principles of fluorescence spectroscopy*. 2013: Springer Science & Business Media.
32. Bhowmick, S., et al., *Resonance energy transfer from a fluorescent dye to a metal nanoparticle*. 2006, AIP.
33. Dulkeith, E., et al., *Fluorescence quenching of dye molecules near gold nanoparticles: radiative and nonradiative effects*. Phys Rev Lett, 2002. **89**(20): p. 203002.
34. Konrad, A., et al., *Strong and Coherent Coupling of a Plasmonic Nanoparticle to a Subwavelength Fabry–Pérot Resonator*. Nano Letters, 2015. **15**(7): p. 4423-4428.
35. Vukovic, S., S. Corni, and B. Mennucci, *Fluorescence Enhancement of Chromophores Close to Metal Nanoparticles. Optimal Setup Revealed by the Polarizable Continuum Model*. The Journal of Physical Chemistry C, 2009. **113**(1): p. 121-133.
36. Pal, P.P. and J. Manam, *Enhanced luminescence of ZnO:RE³⁺ (RE=Eu, Tb) nanorods by Li⁺ doping and calculations of kinetic parameters*. Journal of Luminescence, 2014. **145**: p. 340-350.
37. Beard, M.C., et al., *Multiple Exciton Generation in Colloidal Silicon Nanocrystals*. Nano Letters, 2007. **7**(8): p. 2506-2512.
38. de Chatellus, H.G., et al., *Suppression of Rayleigh scattering noise in sodium laser guide stars by hyperfine depolarization of fluorescence*. Optics Express, 2006. **14**(24): p. 11494-11505.
39. Wang, H., et al., *Influence of excitation power and temperature on photoluminescence in InGaN/GaN multiple quantum wells*. Optics Express, 2012. **20**(4): p. 3932-3940.

40. Peter, J., et al., *Angular dependent light emission from planar waveguides*. Journal of Applied Physics, 2015. **117**(1): p. 015301.
41. Ko, P.J., et al., *Laser Power Dependent Optical Properties of Mono- and Few-Layer MoS₂*. J Nanosci Nanotechnol, 2015. **15**(9): p. 6843-6.
42. Yu, H., et al., *Plasmon-enhanced light-matter interactions and applications*. npj Computational Materials, 2019. **5**(1): p. 45.
43. Sen, T., S. Sadhu, and A. Patra, *Surface energy transfer from rhodamine 6G to gold nanoparticles: A spectroscopic ruler*. Applied Physics Letters, 2007. **91**(4): p. 043104.
44. Chance, R.R., et al., *Fluorescence and energy transfer near interfaces: The complete and quantitative description of the Eu⁺³/mirror systems*. The Journal of Chemical Physics, 1975. **63**(4): p. 1589-1595.
45. Luo, Y., et al., *Plasmonic coupling in single flower-like gold nanoparticle assemblies*. Progress in Natural Science: Materials International, 2016. **26**(5): p. 449-454.

Figures

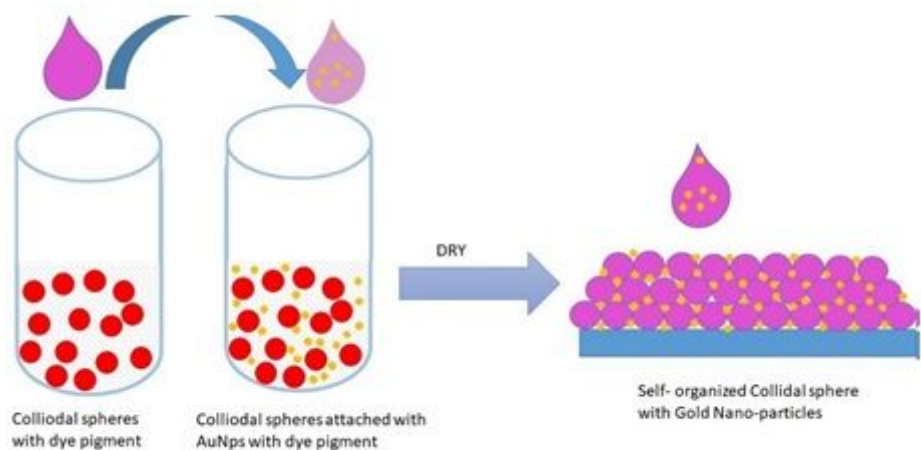


Figure 1

Schematic diagram of the fabrication process and attachment of Au-NPs with self-colloidal spheres.

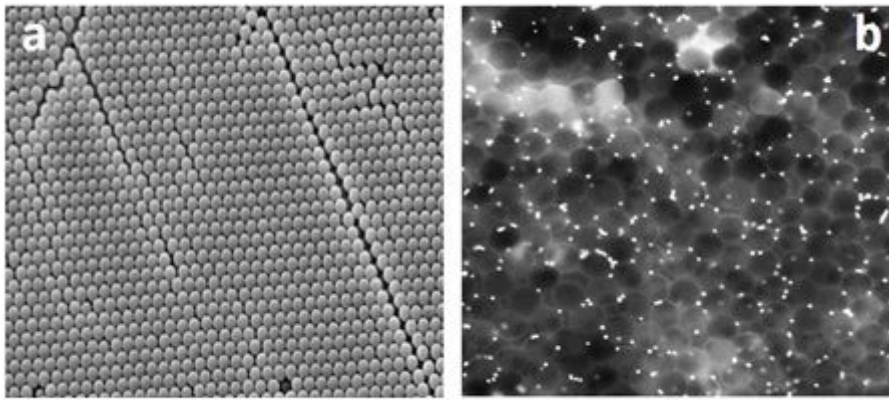


Figure 2

SEM micrograph: PMMA Rh6G spheres (300 nm) and attached with gold nanoparticles 20 nm (a), and (b).

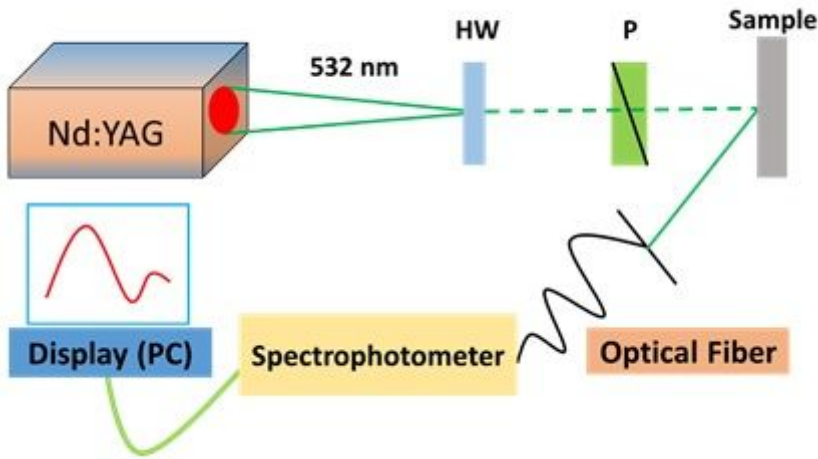


Figure 3

Schematic diagram of the laser set-up for measurements

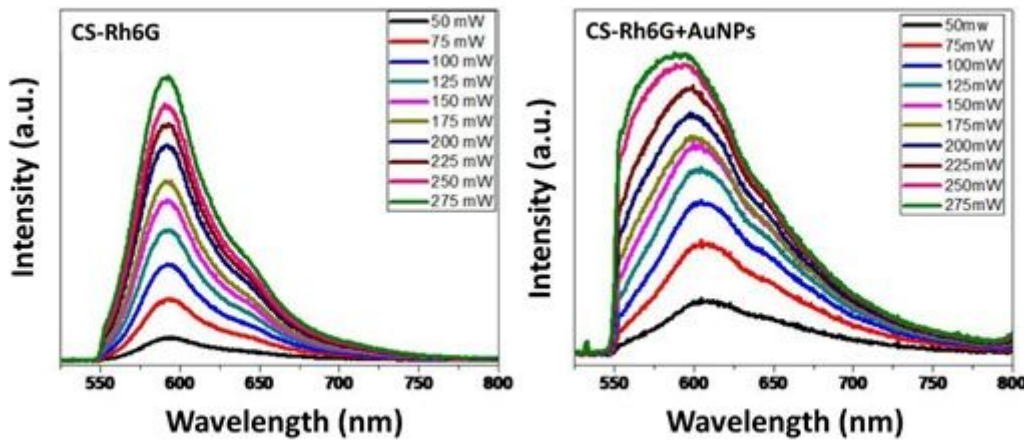


Figure 4

PMMA CS with dye molecule emission spectrum at different powers showing the variation of PL spectra of PMMA CS + AuNPs with various excitation powers of the laser.

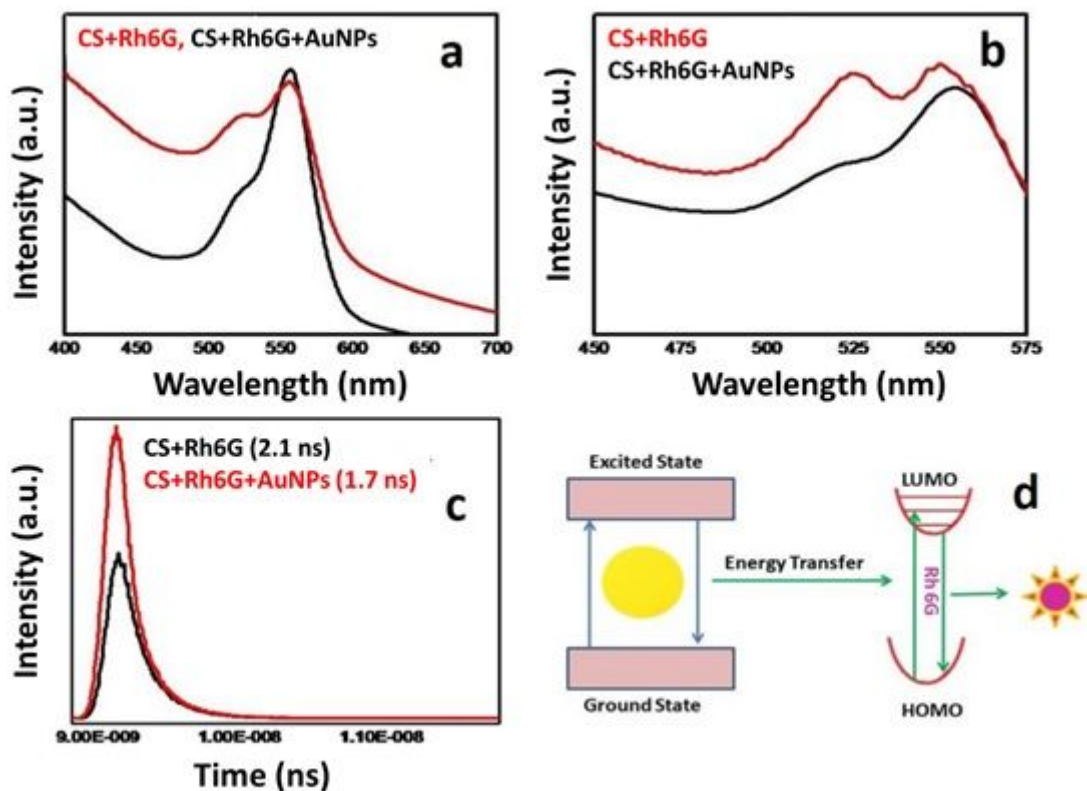


Figure 5

Experimental and simulation study of absorption spectrum CS-Rh6G and CS-Rh6G AuNPs (a and b). Simulation studies and experimental data are following each other and show a good fitting. The distinct gold surface plasmonic peak is observed at ~522 nm in gold attached samples (c). Time-resolved fluorescence spectrum of the Rh6G-CS and presence of AuNPs, and energy transfer diagram (d).